Electromagnetic shielding effectiveness of polycarbonate/graphene nanocomposite foams processed in 2-steps with supercritical carbon dioxide

G. Gedler, M. Antunes, J.I. Velasco, R. Ozisik

www.elsevier.com

PII: S0167-577X(15)30269-X
DOI: http://dx.doi.org/10.1016/j.matlet.2015.07.070
Reference: MLBLUE19268

To appear in: *Materials Letters*

Received date: 11 July 2015
Accepted date: 15 July 2015

Cite this article as: G. Gedler, M. Antunes, J.I. Velasco and R. Ozisik, Electromagnetic shielding effectiveness of polycarbonate/graphene nanocomposite foams processed in 2-steps with supercritical carbon dioxide *Materials Letters,* http://dx.doi.org/10.1016/j.matlet.2015.07.070

Electromagnetic shielding effectiveness of polycarbonate/graphene nanocomposite foams processed in 2-steps with supercritical carbon dioxide

G. Gedler,[a,b] M. Antunes,[a] J.I. Velasco,[a*] R. Ozisik[b,c*]

[a]Centre Català del Plàstic, Departament de Ciència dels Materials i Enginyeria Metal·lúrgica, Universitat Politècnica de Catalunya · BarcelonaTech (UPC). C/Colom 114, E-08222 Terrassa (Barcelona), Spain.

[b]Department of Materials Science and Engineering and [c]Rensselaer Nanotechnology Center, Rensselaer Polytechnic Institute, Troy, NY 12180, U.S.A.

Abstract: The electromagnetic interference (EMI) shielding properties of polycarbonate/graphene composites foamed with supercritical carbon dioxide were investigated as a function of cellular morphology and graphene particle dispersion. The 2–step foaming method used was found to improve graphene dispersion and led to a different cellular structure compared to traditional 1–step foaming. Reflection was found to be the dominant EMI shielding mechanism and EMI shielding effectiveness was improved with large cell morphology that promoted isotropic/random orientation of graphene particles. A maximum EMI specific shielding effectiveness of ~78 dB.cm^3/g was achieved in foams, which was more than 70 times higher that of the unfoamed polymer (1.1 dB.cm^3/g). The study shows that by controlling foaming process conditions and nanoparticle characteristics, it is possible to improve multiple properties while achieving lightweight materials suitable for various applications.

Keywords: Porous materials, polymeric composites, graphene, X-ray techniques, electron microscopy.

[*] Corresponding authors: R. Ozisik (Voice: +1-518-2766786, Fax: +1-518-2768554, E-mail: ozisik@rpi.edu) and J.I. Velasco (Voice: +34 937837022, Fax: +34 937841827, E-mail: jose.ignacio.velasco@upc.edu).

1 Introduction

The preparation of electromagnetic interference (EMI) shielding materials has obtained an increased attention in the academic and industrial fields compared to conventional metal-based EMI materials [1]. Materials with this property are needed for protecting electronics from unwanted radiated signals which can cause unacceptable system performance. The malfunction of electronics can be hazardous, as electronics can be associated with strategic systems such as aircrafts, nuclear reactors, transformers, control systems, communication systems, among others [2]. Nowadays the main goal is to prepare lightweight materials with electromagnetic protection properties [3]. Therefore weight reduction increases the importance for foaming polymers for these types of applications. In the current study we present the effect of the cellular structure promoted by foaming on graphene nanoplatelets orientation and their role on electromagnetic interference shielding behavior.

2 Experimental

Bisphenol A polycarbonate (melt flow index of 17.5 dg/min) and graphene nanoplatelets (GnP) (with average thickness of 6–8 nm, average platelet diameter of 15 μm, and bulk density of 2.2 g/cm^3) were used. Polycarbonate/graphene (PC/GnP) composite samples were prepared by melt compounding using an internal mixing with a graphene concentration of 0.5% (by weight). The pelletized composites were compression–molded in a hot–plate press at 220 ºC at a constant pressure of 4.5 MPa [4]. Foaming was done with the use of supercritical carbon dioxide (CO_2) via a 2–step method as follows: First the samples were saturated in a high–pressure vessel at 80 ºC and 14.0 MPa for 210 min, then they were cooled to room temperature in approximately one hour, followed by slow depressurization. Samples were then removed from the vessel and left to stabilize at room temperature for 120 min. Finally, the samples were heated in a

compression press to 165 ºC for 40, 60, 80 or 100 s at a constant pressure of 6.0 MPa, after which the applied pressure was quickly removed leading to free expansion of the sample [5].

Small and wide angle X–ray scattering experiments were carried out at room temperature on a Nanostar-U instrument (sample distance of 105 cm). Composite morphologies were previously characterized using a JEOL JSM-5610 scanning electron microscope (15 kV, working distance of 30 mm) [4]. The average cell sizes (ϕ) along the disc thickness (vertical direction, ϕ_{VD}) and disc width (radial direction, ϕ_{WD}) were measured using the intercept counting method [6]. The transmission electron microscopy (TEM) images were acquired on a JEOL JEM-2011 LaB6 TEM operating at 200 kV. The electromagnetic interference shielding effectiveness (EMI–SE) measurements were carried out in the X–band frequency range (8.0–12.4 GHz) using an Anritsu 37397C vector network analyzer. The electromagnetic interference shielding effectiveness (EMI–SE) measurements were carried out in the X band frequency range (8.0–12.4 GHz) using an Anritsu 37397C vector network analyzer (VNA), which consisted of two test fixture ports connected to two WR 90 coaxial waveguides and a sample holder that was placed between the two waveguides. Samples were cut to fit into waveguide sample holder (22.9x10.2 mm) with thicknesses of 2 mm. A two port VNA calibration was performed before data collection. Scattering parameters S_{11} (forward reflection coefficient) and S_{21} (forward transmission coefficient) were collected to calculate the electromagnetic interference shielding effectiveness.

3 Results and Discussion

The change of particle morphology after foaming was investigated via TEM. Unfoamed composite (PC–GnP, Figure 1a) presented thicker platelets when compared to foamed samples (Figure 1b) suggesting that there is a partial exfoliation of graphene platelets after foaming.

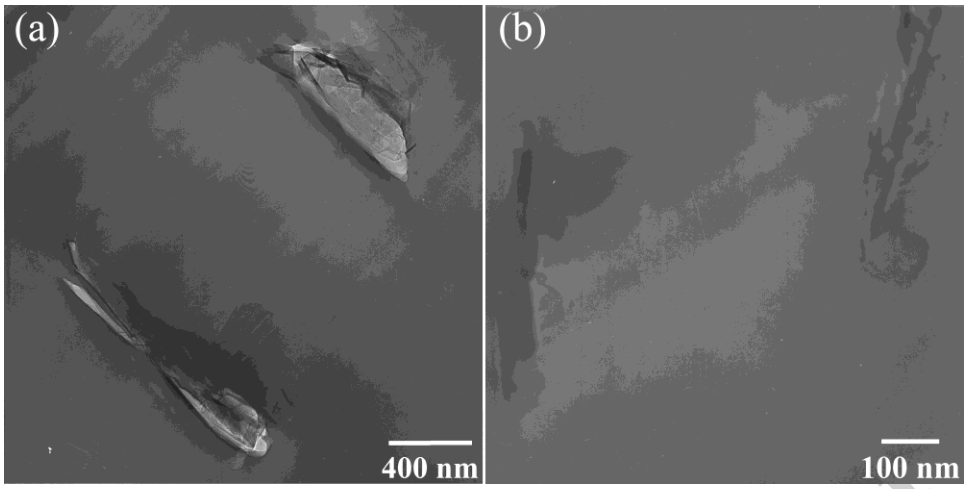

Figure 1. TEM micrographs of (a) unfoamed (PC–GnP) and (b) foamed (PC80–GnP1) composites.

The cellular morphological features of foamed composites, which were discussed in detail in our previous publication [7], were found to depend on the presence of graphene, amount of dissolved supercritical CO_2, and CO_2 saturation/foaming conditions (see Table 1 for a summary).

Table 1. Foaming process parameters and structural features of polycarbonate–graphene composite foams.

Label	t_{heat} (s)	ρ (g/cm^3)	ρ_{rel}	N_f (cell/cm^3)	ϕ_{VD} (μm)	ϕ_{WD} (μm)	*AR*
PC80–GnP1	40	0.18	0.14	6.07×10^8	26	21	1.3
PC80–GnP2	60	0.23	0.19	6.19×10^7	46	34	1.4
PC80–GnP3	80	0.29	0.24	7.88×10^8	20	14	1.4
PC80–GnP4	100	0.33	0.28	1.56×10^9	11	11	1.1

t_{heat}: Heating time; ρ: density; ρ_{rel}: relative density (normalized by the unfoamed composite density of 1.14 g/cm^3); N_f: cell density; ϕ_{VD}: Average cell size along the vertical direction (sample thickness); ϕ_{WD}: Average cell size along the sample width (radial direction); *AR*: aspect ratio ($=\phi_{VD}/\phi_{WD}$).

SAXS experiments showed the presence of structural anisotropy as a function of heating time (Figure 2a–2e). Unfilled PC foamed under the same conditions also showed a similar dependence of anisotropy on heating time suggesting that chain stretching due to cell growth

might have an influence on he anisotropy. However, the anisotropy is stronger in GnP-filled composites suggesting that there might also be a contribution coming from graphene platelets. Two different sets of peaks were observed in SAXS intensity vs. azimuthal angle plots (one pair of peaks at 0º and 180º and the second pair at 90º and 270º) for PC80-GnP4. The locations of these sets of peaks suggest the presence of bimodal orientation [8], which might be explained by the stretching of polymer chains and re-alignment of graphene platelets due to foaming [9] particularly if the cell growth or sample expansion is not isotropic, which is the case in the current study. TEM experiments showed different graphene platelet orientations between samples heated for 100 s (Figure 2f) and 40 s (Figure 2g), which supports that graphene platelets

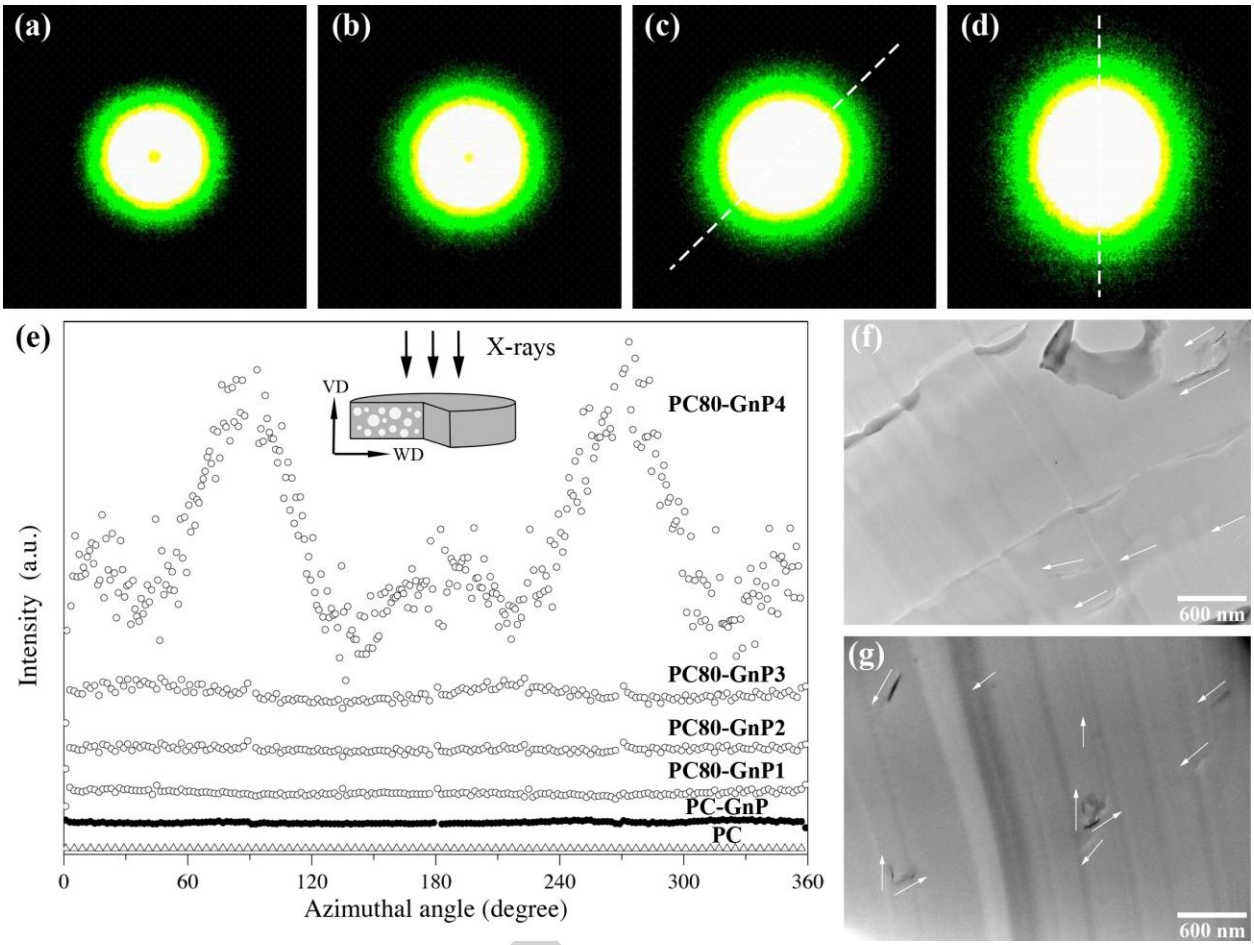

Figure 2. 2D SAXS patterns of (a) PC80–GnP1, (b) PC80–GnP2, (c) PC80–GnP3, and (d) PC80–GnP4 along with their azimuthal distribution of 2D SAXS intensity. Arrows in TEM images of (f) PC80–GnP4 and (g) PC80–GnP1 indicate graphene particle orientations.

might be orienting along the direction of greater expansion (vertical direction); the ratio of vertical expansion (ER_{VD}) to radial expansion (ER_{WD}) was 1.12 for heating time of 40 s and 1.33 for heating time of 100 s. It is, therefore, possible that unequal sample expansions led to both polymer chain stretching and graphene platelet orientation along the vertical direction during foaming (regardless the isotropic-like cellular structure displayed). It is important to note that because of the plasticizing effect of CO_2, the glass transition temperature of PC would be lowered leading to increased mobility [10,11], which would enable chain stretching and orientation of the graphene platelets. However, what we probably observe in azimuthal SAXS

intensity profiles is the contribution coming from structures that have a component along the radial direction (given that the X-ray source was directed along the vertical direction, see inset). Therefore, any anisotropy observed in 2D SAXS patterns observed in Figure 2e should be attributed to graphene orientation due to unequal expansion of the sample.

The EMI shielding effectiveness (EMI–SE) of solid and foamed PC/GnP composites as a function of frequency are presented in Figure 3a. In general, foamed samples showed up to 10 times enhancement in EMI–SE compared to unfoamed composite (PC–GnP). It has been suggested that specific EMI–SE (EMI–SE normalized by density) might be more appropriate when comparing different types of materials such as polymers and polymer foams to metals [12]. In the current study, the greatest specific EMI–SE was found to be ~78 dB.cm^3/g, which is more than seven times greater than that of typical metals (i.e., 10 dB.cm^3/g for solid copper [13]).

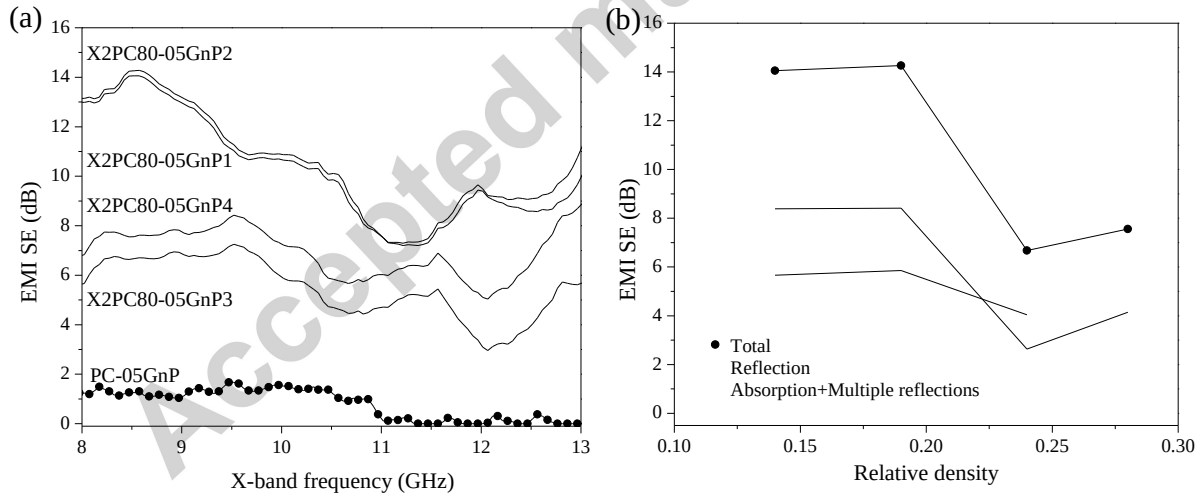

Figure 3. (a) EMI shielding effectiveness of PC/GnP composites and their foams, and (b) contribution of various EMI–SE mechanisms as a function of relative density of foamed composites at a frequency of 8.5 GHz.

EMI–SE showed a dependency on foam relative density, which might suggest that larger cells are desired for achieving better electromagnetic shielding. However, when different shielding mechanisms were investigated separately, it was seen that only reflection contribution

showed a dependency on relative density, and it was by far the most dominant shielding mechanism (Figure 3b). Interestingly, EMI–SE did not shown any perceptible dependency on other structural features such as structural anisotropy probably because it did not alter the structure to affect shielding mechanisms. For example, if a percolated graphene network was formed during foaming, it could have drastically influenced the EMI–SE via adsorption.

4 Conclusions

Electromagnetic interference shielding effectiveness was found to increase 10 times in foamed composites compared to unfoamed composite with the major contribution being the reflection mechanism, and it depended on cellular morphology in a complex manner. Experimental findings suggest that if the expansion of sample is not isotropic during foaming, chains and graphene particles could have preferential orientation along the greater expansion direction (vertical direction in the current study) and as a result, incoming EM waves (directed along the vertical direction) would see a smaller total graphene surface area from which they could be reflected. Therefore, EMI–SE was improved when graphene particles were randomly oriented. Foamed composites also showed a specific EMI–SE of ~78 $dB.cm^3/g$, which is more than seven times higher that of solid copper. Foaming not only reduces density but also was found to impact multiple properties by improving nanofiller dispersion and could lead to the use of these materials in new applications.

5 Acknowledgements

Financial support was provided by the Spanish Ministry of Economy and Competitiveness (MAT2011-26410) and the National Science Foundation (CMMI-1200270, DUE-1003574, DUE-1406405).

6 References

[1] Zhou H, Wang J, Zhuang J, Liu Q. Synthesis and electromagnetic interference shielding effectiveness of ordered mesoporous carbon filled poly(methyl methacrylate) composite films. RSC Advances. 2013;3:23715-21.
[2] Geetha S, Satheesh Kumar KK, Rao CRK, Vijayan M, Trivedi DC. EMI shielding: Methods and materials—A review. Journal of Applied Polymer Science. 2009;112:2073-86.
[3] Park JG, Louis J, Cheng Q, Bao J, Smithyman J, Liang R, et al. Electromagnetic interference shielding properties of carbon nanotube buckypaper composites. Nanotechnology. 2009;20:415702.
[4] Gedler G, Antunes M, Realinho V, Velasco JI. Novel polycarbonate-graphene nanocomposite foams prepared by CO 2 dissolution. IOP Conference Series: Materials Science and Engineering. 2012;31:012008.
[5] Gedler G, Antunes M, Velasco JI. Polycarbonate foams with tailor-made cellular structures by controlling the dissolution temperature in a two-step supercritical carbon dioxide foaming process. The Journal of Supercritical Fluids. 2014;88:66-73.
[6] Sims G, Khunniteekool C. Cell Size Measurement of Polymeric Foams. Cell Polym. 1994;13:137-46.
[7] Gedler G, Antunes M, Velasco JI. Effects of graphene nanoplatelets on the morphology of polycarbonate–graphene composite foams prepared by supercritical carbon dioxide two-step foaming. The Journal of Supercritical Fluids. 2015; DOI:10.1016/j.supflu.2015.02.005.
[8] Laiho A, Hiekkataipale P, Ruokolainen J, Ikkala O. Directing the Smectic Layer Orientation by Shear Flow in Hierarchical Lamellar-within-lamellar Liquid Crystalline Diblock Copolymers. Macromolecular Chemistry and Physics. 2009;210:1218-23.
[9] Malwitz MM, Lin-Gibson S, Hobbie EK, Butler PD, Schmidt G. Orientation of platelets in multilayered nanocomposite polymer films. Journal of Polymer Science Part B: Polymer Physics. 2003;41:3237-48.
[10] Bao J-B, Liu T, Zhao L, Hu G-H, Miao X, Li X. Oriented foaming of polystyrene with supercritical carbon dioxide for toughening. Polymer. 2012;53:5982-93.
[11] Rodríguez-Pérez MA, Campo-Arnáiz RA, Aroca RF, de Saja JA. Characterisation of the matrix polymer morphology of polyolefins foams by Raman spectroscopy. Polymer. 2005;46:12093-102.
[12] Yang Y, Gupta MC, Dudley KL, Lawrence RW. Novel Carbon Nanotube−Polystyrene Foam Composites for Electromagnetic Interference Shielding. Nano Letters. 2005;5:2131-4.
[13] Shui X, Chung DDL. Nickel filament polymer-matrix composites with low surface impedance and high electromagnetic interference shielding effectiveness. Journal of Elec Materi. 1997;26:928-34.

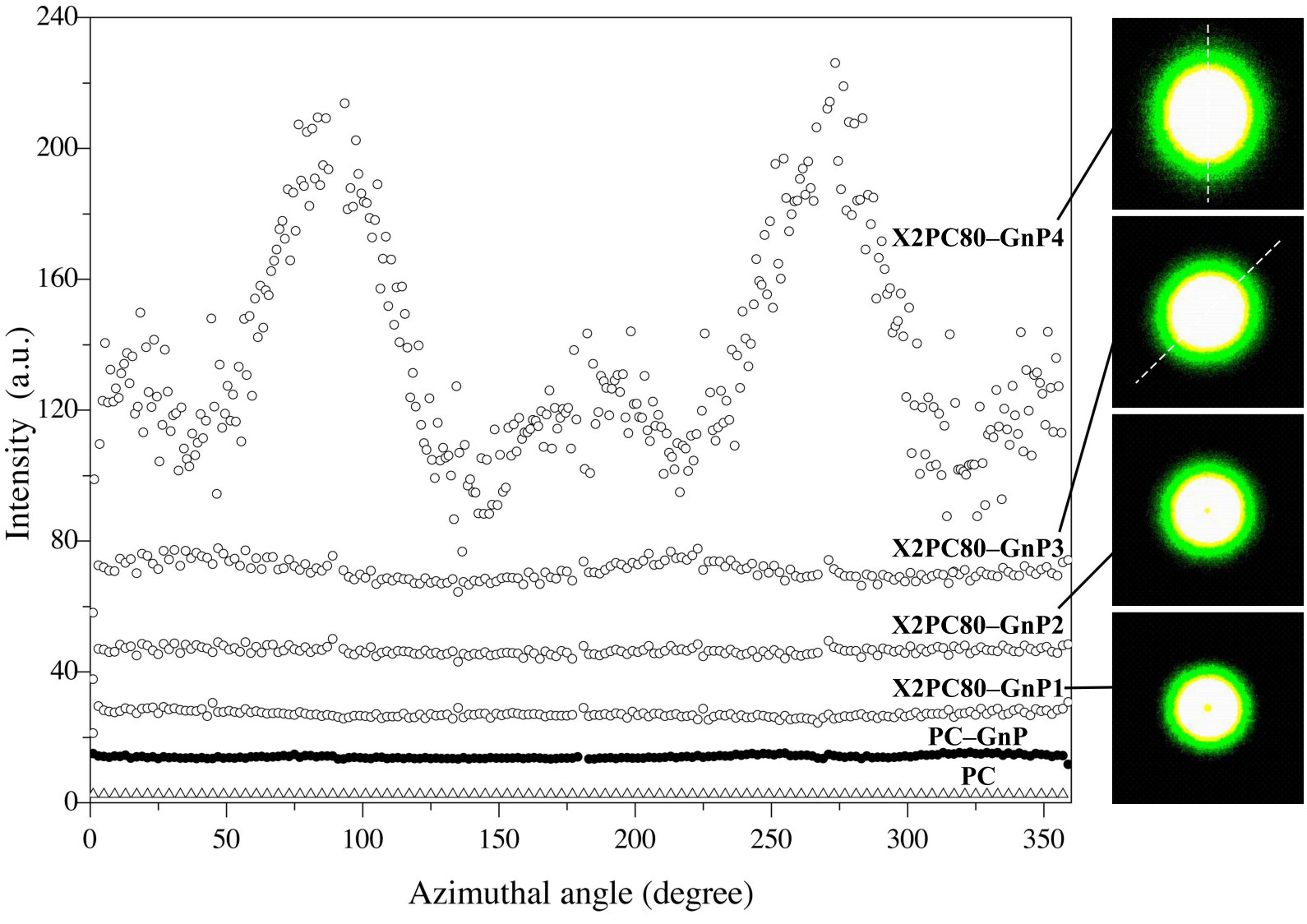

Highlights

- Random orientation of graphene particles improved electromagnetic shielding.
- Larger cells promoted better graphene dispersion/distribution and hence, better EMI shielding.
- Maximum specific shielding effectiveness of foamed composites was 14 dB (78 $dB.cm^3/g$)
- Reflection was found to be the dominant EMI shielding mechanism.
- Shielding effectiveness increased +10 times after foaming.